Alexandria Engineering Journal (2018) 57, 475–481

HOSTED BY

Alexandria University

Alexandria Engineering Journal

www.elsevier.com/locate/aej
www.sciencedirect.com

ORIGINAL ARTICLE

SEM and AFM microscopical characterization of rPAN fibre and PET blends

Adesola Adegbola [a,*], I.E.A. Aghachi [a], Oluranti Sadiku-Agboola [b]

[a] Department of Mechanical Engineering, Faculty of Engineering and the Built Environment, Tshwane University of Technology, Pretoria 0001, South Africa
[b] Department of Chemical Engineering, Faculty of Engineering and the Built Environment, Tshwane University of Technology, Pretoria 0001, South Africa

Received 22 March 2016; revised 27 April 2016; accepted 6 November 2016

KEYWORDS

Recycling;
Blends;
rPAN;
PET;
Compounding and characterization

Abstract Recycling is one of the key ways of improving polymer properties and viable applications. Polymer blends are generating desired properties and the strength of recycled polymer improves depending on the ratio of the compositional blend. Microscopic characterization of the properties of recycled polyacrylonitrile fibre with polyethylene terephthalate using SEM and AFM was investigated in this work. The results revealed that blended compositions of rPAN/PET (50/50; 70/30) are viable to explore while rPAN/PET (30/70) blend resulted in poor adhesion between the matrix and phase. Therefore, high percentage composition of rPAN in the blended samples positively improves the processing properties of PET.

1. Introduction

Polyacrylonitrile (PAN) products are finding application in the field of polymer development due to their high mechanical strengths, toughness and excellent thermal properties [1]. These attributes are very indispensable in understanding PAN functions and its application as precursors for the production of carbon fibre [2,3], etc. Therefore, many PAN products have been discovered for different applications as the need required. These PAN products are not easily disposed and the need for their recycling is coming to light, due to government legislative laws on recycling. Recycling of PAN and PAN blends is challenging because they comprised of multiple segments (matrix and phases). Hence, there has been significant research into the recycling of PAN due to a number of recycling technologies now available [4–6]. Of all the different PAN recycling methods, mechanical recycling is the simplest approach. This process allowed pure and used PAN materials to be compounded with other polymers which are either miscible or immiscible [4,5].

Different recycling techniques have been reported in the work of many authors. Their reports have shown tremendous improvement in blending application of PAN [7–14]. In addition, great effort has also been applied in the blending and development of PET as reported in many journals [15–19]. Little effort is shown in the compatibility of rPAN with PET; hence, the need for this study to be carried out.

* Corresponding author.
E-mail addresses: adesolaat@tut.ac.za (A. Adegbola), funmi2406@gmail.com (O. Sadiku-Agboola).
Peer review under responsibility of Faculty of Engineering, Alexandria University.

http://dx.doi.org/10.1016/j.aej.2016.11.001

In this current study scanning electron microscopy (SEM) and atomic force microscopy (AFM) were used to characterize rPAN, PET and rPAN/PET blended samples. SEM and AFM have proved to be a very useful technique employed for surface imaging with sub-nanometric resolution. By imaging the samples with SEM and AFM, surface topography, composition, molecular structure, pores distribution, surface roughness and morphological aspect local properties, such as height, friction, with a probe were validated [9–11]. These characterizations are highly important in the development of the rPAN/PET blends. This also aided the understanding of the effect of blended ratios composition of the rPAN/PET.

2. Experimental methods

2.1. Materials

The rPAN fibre employed in this study was supplied by ESKOM, South Africa. Neat PAN has a molecular weight (M_w) = 53.06 g/mol, amorphous density of 1.184 g/cm^3. The glass transition and melting temperatures are 95 °C and 317 °C, respectively. The PET was purchased by the Tshwane University of Technology (TUT) from Ten Cate advanced composites BV, the Netherlands. PET has a molecular weight, (M_w) = 192.2 g/mol and the amorphous density of 1.370 g/cm^3. It's glass transition and melting temperatures are 75 °C and 285 °C, respectively.

2.2. The recycled PAN fibre and PET processing

rPAN fibres were cleaned by soaking in water for 12 h, rinsed and dried for 24 h at room temperature in order to remove the ash and coal particles embedded in it before the blending process took place. Dried rPAN fibres and neat PET were prepared through melt blending using the HAAKE Polylab OS Rheomix 600 (Thermo Electron Co., USA) at 290 °C for 5 min with a rotor speed of 80 rpm. The rPAN and PET were blended at the ratios of 30/70, 50/50, and 70/30 as received, while rPAN and PET were used as controls. The resulting blends and control samples were then compression-moulded to the desired dimensions for the various tests, using a carver compression mould (Carver, USA). The total compression residence time of 10 min with a compression step of 2 min at a pressure of one metric ton was employed and water was also used for the slow cooling during the carving process. Table 1 shows the rheomixer operating parameters.

Table 1 Rheomixer operating parameters.

Temperature	290 °C
Speed	60 rpm
Time (min)	5 min
Roller - rotor	600 rpm
Sample mass	25 g
Density	1 g/cm^3

3. Characterization

3.1. Scanning electron microscopy (SEM)

The cryogenically fractured-surface morphology of rPAN, PET and the blended samples was determined using a JEOL-SEM model JSM-7500LV field emission scanning electron microscopy (SEM) (JEOL, Japan). An accelerating voltage of 3 kV was used under the gentle beam (low mode) in order to prevent the beam from damaging the samples. The samples were prepared by immersion in liquid nitrogen, cryogenically-fractured, mounted on stubs edge-on and coated with mercury in order to enhance conductivity. The images were collected at a magnification of 50,000×. The size of the distinct features in the images was determined using ImageJ (National institute of Health, USA).

3.2. Atomic force microscopy (AFM)

Atomic force microscopy (AFM) WSxM 5.0 development 6.4 and digital instruments/VEECO multimode are currently finding wide application in polymer surface imaging topography at high resolution. AFM is designed to acquire images, measure and generate statistical properties such as the height distribution function, the root-mean-square (rms), slope, curvature, average height, average surface area, power spectral density, average surface roughness and surface fractal analysis used to characterize polymer surfaces during analysis. AFM uses scanning probe microscope (SPM) raster-scans over a small area of samples and simultaneously measured the local properties for analysis [20,21]. For this reason the measurement of force curves has become essential in different fields of research, such as surface science and materials engineering [22–24].

In conclusion, AFM does not only measure the force on the polymer sample but also regulate and allow acquisition of images at very low forces. Lastly, a well-constructed feedback loop is essential for AFM to generate 2D and 3D images for detail analysis.

4. Results and discussion

4.1. The blends morphology

The nodule-like structure observed in Fig. 1a is due to the net predominance of the solid-solid demixing during the blending process. This demixing promotes simultaneous nucleation and growth of the blend crystallites in all directions. The nodules characterizing rPAN/PET blends exhibit different size and compactness due to the blending ratio (Fig. 1a–c). In addition, an increase in the processing temperature of PET resulted in spherulite network characterized by the size suggesting that the number of nuclei of crystallites in the blend is reduced at a higher temperature, which favours crystal growth in structure formation. Therefore, changes in the degree of interconnectivity of blends structure are expected according to Gugliuzza and Drioli [25]. In addition, high composition of PET in the blend decreases spherulites number of links, resulting in an increase in the pores formation. The formation of larger and larger gaps between the spherulites generates the blends pores, whose size and distribution are significantly dependent on the blend ratio [25].

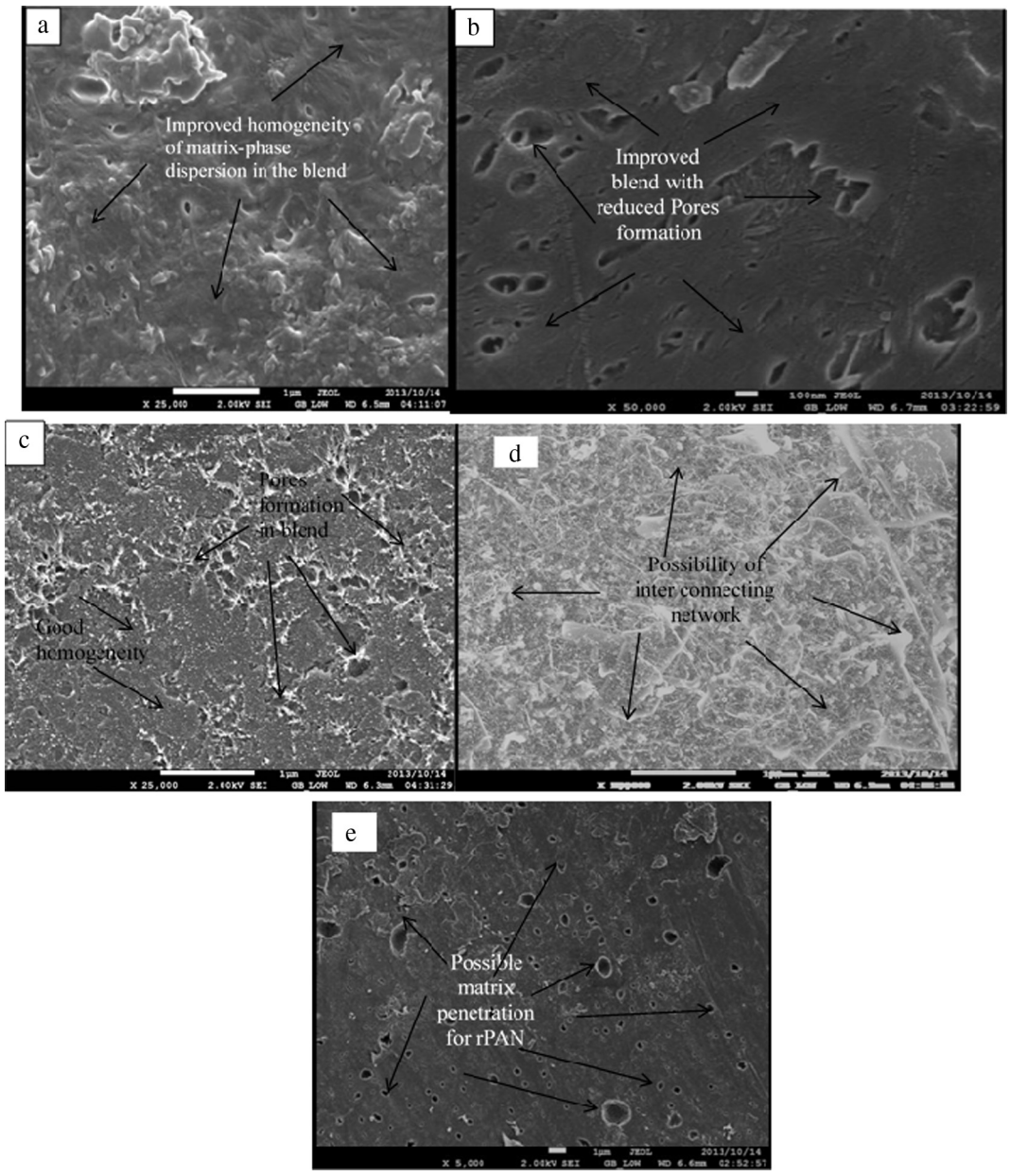

Figure 1 Morphology of freeze-fractured surfaces of: (a) rP AN/PET (70/30), (b) rPAN PET (50/50), (c) rPAN/PET (30/70), (d) rPAN and (e) PET. Images were collected at 50,000× at a voltage of 2 kV.

4.2. Structure-property relationships

Varying the blend ratio and increasing the processing temperature of PET affect the performance of the blended polymers. In the present work, the fraction of PET in the blend was bound to influence the viscosity of rPAN and same as rPAN for PET. Therefore, the morphology of rPAN/PET blends was studied in order to elucidate the blend homogeneity or otherwise validate the correlation between the morphology, pores distribution and blend compositional ratios as follows.

Fig. 1a shows the blend of rPAN/PET (70/30). This blend reveals a near total dispersion of PET in the rPAN matrix. The blend spherulites appear more compacted because of additional interlinks provided by high rPAN composition in the blend. Also, due to high composition of rPAN in the blend, disperse phase decreased remarkably according to Lepers et al. [26]. Therefore, high rPAN composition in the blend reduces PET particle size because the dispersed phase is less viscous than the matrix according to Chesters [27] and Minale et al. [28]. This implies that the compatibility between rPAN and PET increased with increasing rPAN content by reducing the interfacial adhesion between the two components, see Fig. 1a SEM image.

Fig. 1b reveals the morphology of rPAN/PET (50/50) sample. The micrograph shows co-continuous morphology in the blend structure which contains some degree of interpenetrating and self-supporting phases of the rPAN/PET blend. This shows the continuous path through which either phase may

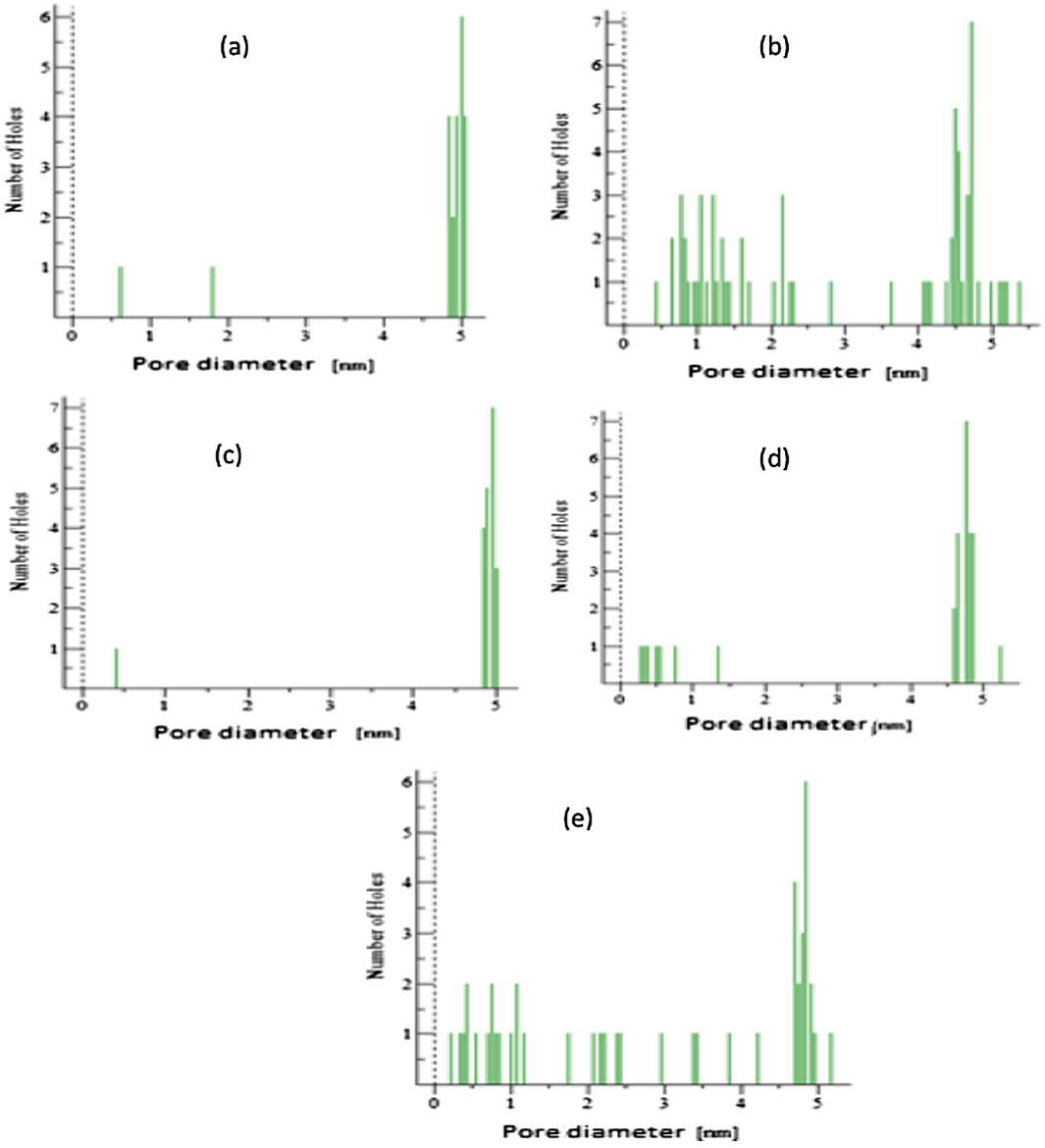

Figure 2 Pore size distribution of (a) rPAN, (b) PET, (c) rPAN/PET (70/30), (d) rPAN/PET (50/50) and (e) rPAN/PET (30/70).

be drawn to the boundaries, although some dispersed phase portions were also observed in the blend.

The morphology of rPAN/PET (30/70) sample is shown in Fig. 1c. The blend shows some degree of uniformity of the two polymers, but it further revealed the formation of pores in the blend which resulted in the matrix weakness, thereby leading to sample brittleness as a result of poor adhesion between the components. This ratio is not viable for recycling processes.

The micrograph of rPAN shows a complex interconnected network of fibres (Fig. 1d). Obviously, the rPAN fibre morphology provides a compounding pathway that can enhance an effective blending and this can improve the rPAN blend properties if carefully explored as shown in the blends of rPAN/PET (70/30 and 50/50). Fig. 1e shows the morphology of the pure PET, and this shows a possible matrix compounding for new material development. The morphology reveals the possibilities of fibre penetration in the network of the matrix; this is a positive prospect for rPAN fibre blending.

Lastly, SEM cryogenically-fractured surfaces of rPAN, PET and rPAN/PET blended samples also revealed pore distribution. This pore size and its distribution are very important for the performance data analysis in recycling technology. It provides a quantitative description of the range of pore sizes present in a given blended sample and it gave a more accurate description of the particle sizes that is likely to affect the blended compositional ratios. Pore size distribution is one of the numerical parameters that can be obtained directly from the AFM.

AFM topography imaging of samples was helpful in obtaining information on the pore size distribution by providing statistics on the surface of pore dimensions (Fig. 2). In the study, the pore size distribution varies with the blended samples compositional ratios, that is, with rPAN as the matrix,

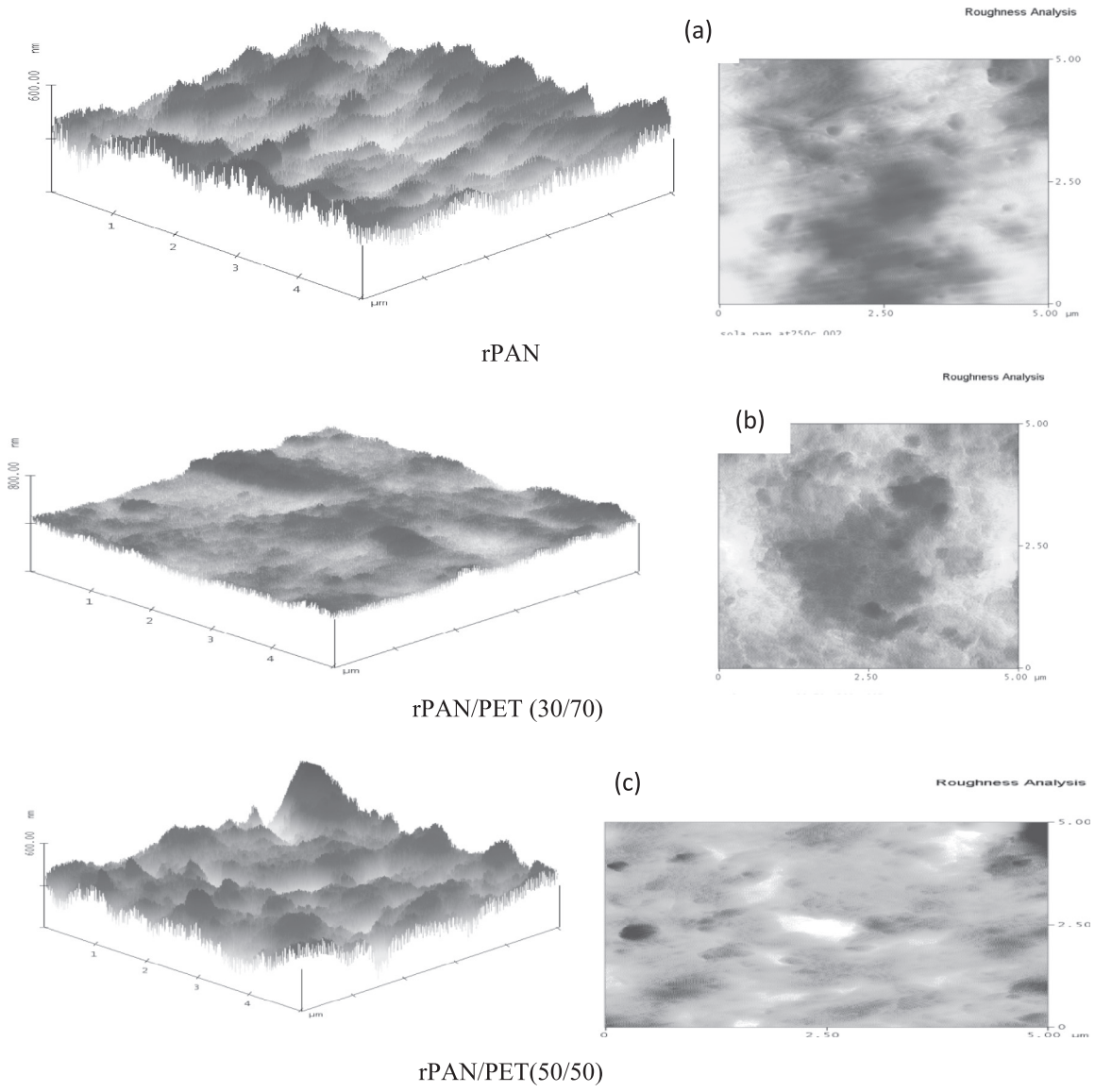

Figure 3 AFM microgram of (a) rPAN, (b) rPAN/PET (30/70), (c) rPAN/PET (50/50), (d) rPAN/PET (70/30) and (e) PET samples.

the pore size distribution decreases (Fig. 2c) while the introduction of PET as matrix increased the pore size distribution in the blend (Fig. 2e). This resulted in poor adhesion between the matrix and phase composition rPAN/PET (30/70) (Fig. 2).

4.3. Surface roughness analysis with atomic force microscopy (AFM)

Fig. 3 shows the non-contact mode 3D topography images obtained from AFM for 5.0 μm × 5.0 μm rPAN, PET and rPAN/PET blended samples. The 3D topography images represent the samples top views with the information on the depth of the samples in the *Z*-direction, coded in colour intensity having the highest points. The light regions represent the peaks and the dark region represents the pores. The samples have a thick structure and higher ridges of three-dimensional orthographic features. These ridges could be due to the incorporated developed programming tool that can be useful when investigating the rPAN/PET blended samples and the thick structure was as a result of the dense nature of the matrix-phase composition. The 3D orthographic image of samples shows the occurrence of tiny peaks and valleys.

The tiny peaks are responsible for the improved roughness of rPAN/PET (50/50 and 30/70) when compared to PET; this might lead to improved adhesion of the matrix and phase [29]. The roughness parameter of the rPAN/PET (70/30) was very low. Furthermore, Table 2 reveals that the roughness values decreased as PET was added to rPAN. This trend resulted in the weakening of the interlinking network of the blends; poor adhesion between the matrix and the phase leads to brittleness. This brittleness was revealed by the cracking of rPAN/PET (30/70) during preparation for further test. In conclusion, the addition of PET above 50% in composition weakens the blend and makes the blend unsuitable for the proposed recycling application. Introduction of suitable additives can be explored to improve this weakness.

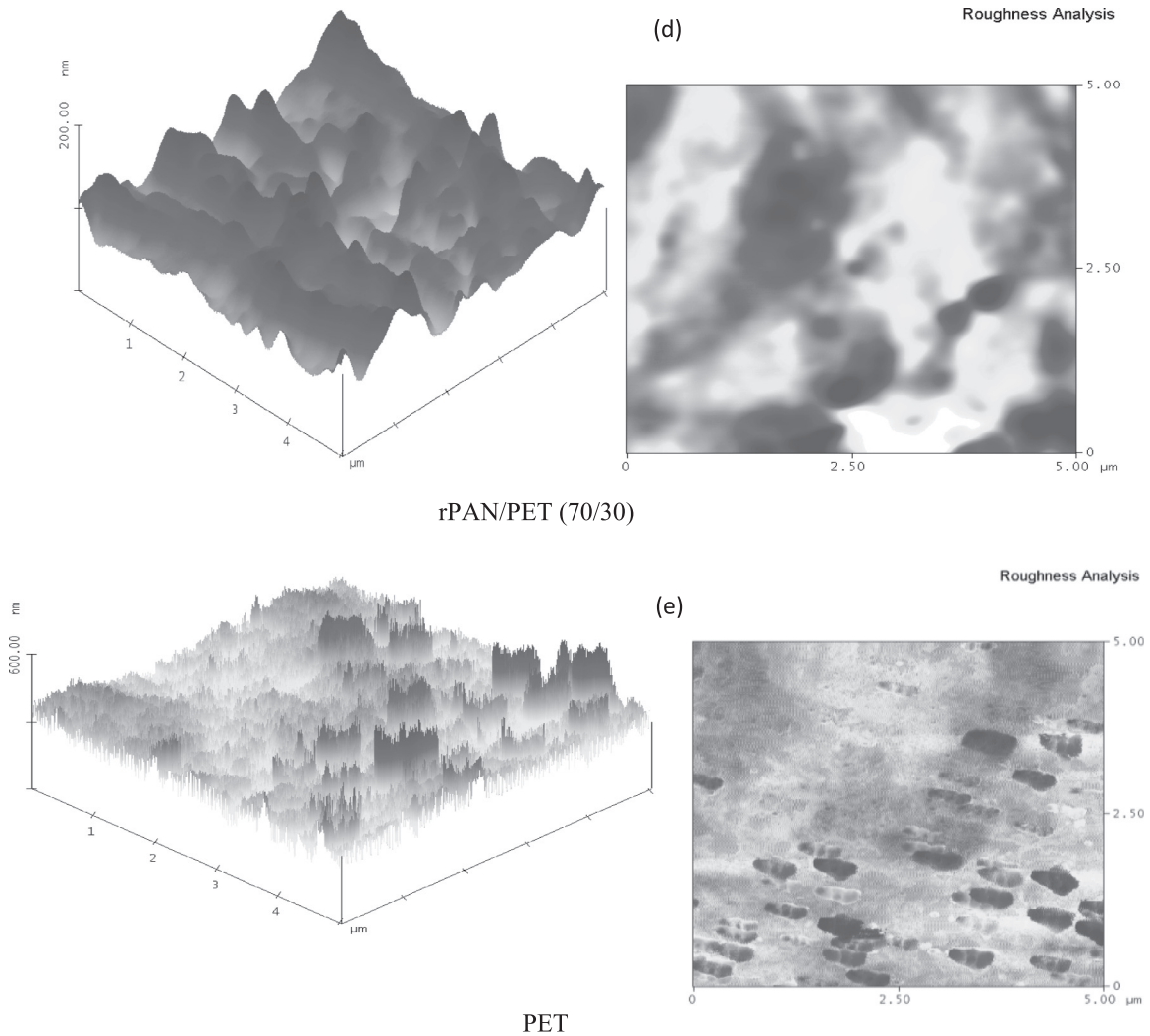

Fig. 3 (*continued*)

Table 2 Summary of AFM roughness analysis.

Sample	Img. Rms (Rq) (nm)	Mean roughness (Ra) (nm)
rPAN (100)	80.304	65.739
rPAN/PET (30/70)	63.232	49.781
rPAN/PET (50/50)	70.371	53.693
rPAN/PET (70/30)	20.924	15.806
PET (100)	49.508	38.698

5. Conclusions

The AFM pore size distribution and surface roughness shed light on the behaviour of rPAN/PET blended samples. This provided valuable information on rPAN/PET blended samples characterization. The study also revealed that rPAN/PET (50/50) is the optimum blended ratio for PET and any ratio above 50% of PET resulted in poor adhesion between the matrix and phase, which lead to the poor blended composition. SEM micrographs showed that, varying the ratio of the blends has a significant effect on the mechanical property. Therefore, both AFM and SEM are significant tools that aided the development of the rPAN/PET blends. In addition, the study also revealed that used PAN can be recycled with PET at different blended ratios.

A further development is the proposed addition of additives and fillers to the composition in order to explore the possible application of the blend of rPAN/PET. This is to improve on the phase separation observed in this current study.

Acknowledgment

ESKOM TESP grant for research support.

References

[1] S. Chand, Carbon fibers for composites, J. Mater. Sci. 35 (2000) 1303–1313.
[2] D.D. Edie, The effect of processing on the structure and properties of carbon fibers, Carbon 36 (1998) 345–362.
[3] Y.V. Basova, D.D. Edie, Y.S. Lee, L.K. Reid, Effect of precursor composition on the activation of pitch-based carbon fibers, Carbon 42 (2004) 485–495.

[4] B.K. Kim, Y.S. Oh, Y.M. Lee, K.Y. Lee, L. Soo, Modified polyacrylonitrile blends with cellulose acetate: blend properties, J. Polym. 41 (2005) 385–390.
[5] D.M. Cates, H.J. White, Preparation and properties of fibers containing mixed polymers. II. Polyacrylonitrile-cellulose fibers, J. Polym. Sci. 20 (1956) 181–195.
[6] W. Pan, S.L. Yang, M.J. Jian, G. Li, Electrical and structural analysis of conductive polyaniline/polyacrylonitrile composites, Eur. Polym. J. 41 (2005) 2127–2133.
[7] M.P. Taylor, Temperature and strain controlled optimization of stabilization of polyacrylonitrile precursor fibers, Theses and Dissertations–Mechanical Engineering, Paper 4, 2012. <http://uknowledge.uky.edu/me_etds/4>.
[8] S.Y. Yun, J.-H. Ha, Y. Kim, W.K. Lee, Process optimization for preparing high performance PAN based carbon fibers, Bull. Korean Chem. Soc. 30 (2009) 6.
[9] J. Liu, P. Zhou, L. Zhang, Z. Ma, J. Liang, H. Fong, Thermo-chemical reactions occurring during the oxidative stabilization of electrospun polyacrylonitrile precursor nanofibers and the resulting structural conversions, Carbon 47 (2009) 1087–1095.
[10] Y. Liu, H.G. Chae, S. Kumar, Stabilization of Gel-Spun Polyacrylonitrile/Carbon Nanotubes Composite Fibers. Part II: Stabilization Kinetics and Effects of Various Chemical Reactions, School of Polymer, Textile and Fiber Engineering. Georgia Institute of Technology, Atlanta, 2010.
[11] M.J. Yu, C.G. Wang, Y.J. Bai, N. Lun, Y.-X. Wang, B. Zhu, Evolution of tension during the thermal stabilization of polyacrylonitrile fibers under different parameters, J. Appl. Polym. Sci. 102 (2006) 5500–5506.
[12] Y.-J. Bai, C.-G. Wang, N. Lun, Y.-X. Wang, M.-J. Yu, B. Zhu, HRTEM. Microstructures of PAN precursor fibers, Carbon 44 (2006) 1773–1778.
[13] M. Rahaman, A. Ismail, A. Mustafa, A review of heat treatment on polyacrylonitrile fiber, Polym. Degrad. Stab. 92 (2007) 1421–1432.
[14] S. Dalton, F. Heatley, P.M. Budd, Thermal stabilization of polyacrylonitrile fibers, Polymer 40 (1999) 5531–5543.
[15] X. Fei, E.A. Lofgren, A.J. Saleh, Melting and crystallization behaviour of poly (ethylene terephthalate) and poly (m-xylylene adipamide) blends, J. Appl. Polym. Sci. 118 (2010) 2153–2164, VC 2010 Wiley Periodicals, Inc..
[16] M.C. Costache, M.J. Heidecker, E. Manias, C.A. Wilkie, Preparation and characterization of poly (ethylene terephthalate)/clay nanocomposites by melt blending using thermally stable surfactants, J. Polym. Adv. Technol. 17 (2006) 764–771.
[17] C.F. Ou, M.T. Ho, J.R. Ling, Synthesis and characterization of poly (ethylene terephthalate) nanocomposites with organoclay, J. Appl. Polym. Sci. 91 (2004) 140–145.
[18] Y. Imai, Y. Inukay, H. Tateyama, Properties of poly (ethylene terephthalate)/layered silicate nanocomposites prepared by two-step polymerization procedure, J. Polym. 35 (2003) 230–235.
[19] C.H. Davis, L.J. Mathias, J.W. Gilman, D.A. Schiraldi, J.R. Shields, P. Trulove, T.E. Sutto, H.C. Delong, Effects of melt-processing conditions on the quality of poly (ethylene terephthalate) montmorillonite clay nanocomposites, J. Polym. Sci. Part B 40 (2002) 2661–2666.
[20] G.K. Pang, K.Z. Baba-Kishi, A. Patel, Topographic and phase contrast imaging in atomic force microscopy, Ultramicroscopy 81 (2000) 35–40.
[21] G. Bar, L. Delineau, R. Brandsch, M. Bruch, M.-H. Whangbo, Importance of the indentation depth in tapping-mode atomic force microscopy study of compliant materials, Appl. Phys. Lett. 75 (1999) 4198–4200.
[22] G. Bar, R. Brandsch, Effect of viscoelastic properties of polymers on the phase shift in tapping mode atomic force microscopy, Langmuir 14 (1998) 7343–7347.
[23] J.P. Cleveland, B. Anczykowski, A.E. Schmid, V.B. Elings, Energy dissipation in tapping mode atomic force microscopy, Appl. Phys. Lett. 72 (1998) 2613–2615.
[24] H.-J. Butt, B. Cappella, M. Kappl, Force measurements with the atomic force microscope: technique, interpretation and applications, J. Surf. Sci. Rep. 59 (2005) 1–152.
[25] A. Gugliuzza, E. Drioli, New performance of hydrophobic fluorinated porous membranes exhibiting particulate-like morphology, Desalination 240 (2009) 14–20.
[26] J.-H. Lepers, B.D. Favis, C. Lacroix, J. Polym. Phys. 37 (1999) 939–951.
[27] A.K. Chesters, Trans. I Chem. E 69 (1991) 259.
[28] M. Minale, P. Moldenaers, J. Mewis, Macromolecules 30 (1997) 5470.
[29] W.R. Bowen, N. Hilal, R.W. Lovitt, C.J. Wright, J. Membr. Sci. 139 (1998) 269.